Determination of Transmission Coefficients and Energy Density of an Overlay Microstrip Patch Antenna for Microwave Filters and Feeds Designs Using Microwave Methods

Abubakar Yakubu[1*], Zulkifly Abbas[2] and Suleiman Sahabi[3]

[1]*Department of Physics, Kebbi State University of Science and Technology, Aliero, Nigeria.*
[2]*Department of Physics, University Putra Malaysia, Serdang, Selangor, Malaysia.*
[3]*Faculty of Science, Kebbi State Polytechnic, Dakingari, Nigeria.*

Authors' contributions

Article Information

Original Research Article

ABSTRACT

In designing filters and antenna feeds at microwave frequency, the energy density and stop bands are of vital importance. To this development, this work is set out to determine the transmission coefficients behavior of substrates along with their energy density for a microstrip structure using finite element method (FEM) and Vector network analyzer (VNA). In this work, a 15, 30 and 50 mm PTFE samples were used as an overlay substrate material on a patch microstrip antenna. Simulations and measurement were then carried using FEM and VNA, respectively. Transmission coefficient obtained via FEM and VNA were compared and the behavior of the substrates at 10 GHz were noted which is the area of broad stop band. Results from simulation and measurement showed that the energy density of the 50 mm thick substrates was 1.67×10^{-5} J/m^3 while the

---

*Corresponding author: Email: abulect73@yahoo.com;*

attenuated power for the 15, 30 and 50 mm thick substrates at 10 GHz were 6.8, 8.0 and 14.6 dB, respectively. Based on these findings, it is concluded that the 50 mm thick PTFE substrates has the deepest stopband at 10 GHz and more suitable for filter designs and antenna feeds.

1. INTRODUCTION

Knowledge of materials behaviour placed in an electromagnetic field is of immense importance especially when it relates to military hardware, electronics, communication and industrial applications [1]. The measurement of S parameters of materials in the microwave frequency range is found in numerous areas. A good understanding of the S-parameter measurement of these materials is necessary to get useful information from materials proposed for use in microwave absorption.

The benefits of microstrip structures, also referred to as electromagnetic bandgap structures, have been discussed often in the past years [2]. The motivations for using substrates can be classified in two categories: eliminating substrate modes in antenna applications, and in guided-wave filters. Mostly, substrates are used in microstrip lines for widening and absorption of scattered waves and achieving more compact circuits [3]. Microstrip lines have been reported severally by a number of researcher's [3]. Most microstrip antennas are replicas of the one shown in Fig. 1, however, designs and conventions may differ.
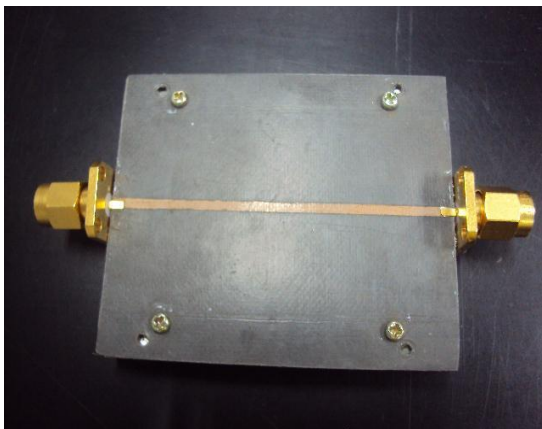
Fig. 1. Open microstrip antenna

The slotted lines in the antennas are made by etching on the ground plane of the microstrip. The slots vary in shape from round to almost rectangular for modifying the propagation and

guided wave stopband shape [4,5]. In literature, the insertion and return loss of these filter structures has been successfully analyzed, designed and implemented [6]. Over the years, numerous methods have been used to calculate the S parameters of samples at microwave frequency. However, to the best of our knowledge, energy density radiation imaging from slotted-ground plane microstrip structures has not been reported.

For this reason, this work is targeted in using Finite Element method (FEM) in the simulation and visualization of transmission coefficient and energy density of slotted line microstrip antenna. For ease of work and calculations, 3D simulation may be used to replace the need for complex theoretical analysis of the measurement geometry. The substrate used in this work is PTFE (Teflon) for all measurements and calculations. Teflon was used in this study because it has a standard value of permittivity which would be used in the simulation. The permittivity value of Teflon used in the simulation is 2.04.

2. THEORY OF SCATTERING PARAMETER (FEM)

Scattering parameters S_{11} and S_{21} can be calculated from the reflection and transmission coefficients of an overlay microstrip using the signal flow graph analysis as reported in [7],

$$S_{11} = S_{22} = \frac{\gamma(1 - Z^2)}{1 - \gamma^2 Z^2} \quad (1)$$

$$S_{21} = S_{12} = \frac{Z(1 - \gamma^2)}{1 - \gamma^2 Z^2} \quad (2)$$

Where.

$$\gamma = \frac{Z_s - Z_0}{Z_s + Z_0} \quad (3)$$

$$Z = -jesp(\gamma l) \quad (4)$$

Where

Z_s, Z_0, l and γ are characteristic impedance of the measurement system, input impedance,

sample length and propagation constant, respectively.

For the simulation, the solution time to calculate the S_{11} and S_{21} using COMSOL is strongly influenced by mesh properties such as geometry conformity, mesh density and element quality. Sufficient approximation of the problem domain is required for the geometry conformity of the area defined by the mesh elements. Minimization of the discretization error and achieving accurate solutions can be assured by having the mesh with density and size that are sufficiently high and small respectively. Thus, it is a good option to use denser mesh which is having smaller elements in the regions, where a high spatial variation of the investigated fields is anticipated. In this work, unstructured meshes are employed.

The finite element method leads to a linear equation system solved iteratively. Automatic mesh adaptation and improvement based on the refinement in the regions that prevents the highest error in the approximation procedure is used throughout the computational process. Usually, when the number of FEM mesh elements increases, the accuracy of the computational result also increases. Finer mesh will increase the number of initial mesh elements for the microstrip sensor and as a consequence higher number of degrees of freedom solved.

About 10 different solver options are provided by COMSOL to reduce the computational time. The SPOOLES solver is selected in this work due to its high computational speed and low RAM (random access memory) requirement, typically about 2.0 GB. Shown in Fig. 2 is a simulation of a meshed overlay microstrip antenna in 3-dimension using FEM.
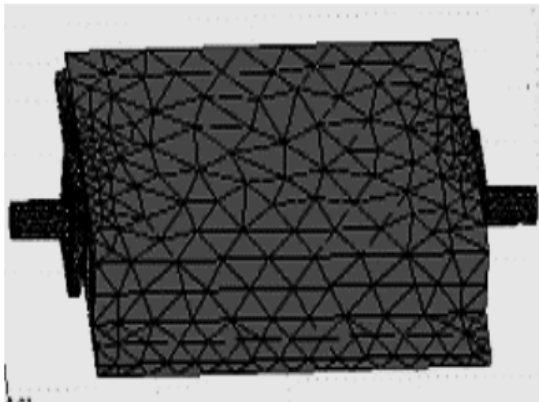

Fig. 2. Meshed overlay microstrip antenna

3. METHODOLOGY

3.1 FEM Simulation

The first step in our work was to calculate the values of S_{11} and S_{21} using the COMSOL software version 4.5b. For the case of simulation, the radiation is simulated in two ways. In the first case, the wave equation is integrated through the radiation boundary box in the finite element simulator. In the second case, the energy density and attenuated power were calculated from the transmitted coefficients.

For the simulation, the wave equation shown in (5) is used [8];

$$\nabla x \left(\mu_r^{-1} \nabla x E_z\right) - \left(\varepsilon_r - j\frac{\sigma}{w\varepsilon_0}\right) k_0^2 E_z = 0 \quad (5)$$

where;

μ_r is relative permeability, k_o is free pace wave number, j is imaginary unit, σ is conductivity, w is angular frequency, ε_r is relative permittivity and ε_o is permittivity of air.

In the COMSOL environ, we first of all assign our work in the 3D work plane before going into the RF module where electromagnetic wave is selected for harmonic waves. When all parameters have been rightly assigned, the microstrip with an overlay substrate of 15, 30 and 50 mm thicknesses and slot line radius of 2.5 mm is meshed with high mesh density. The result of the transmission coefficients and total energy density at 201 steps between 8 to 12 GHz is calculated and visualized, respectively.

3.2 Measurement Using Vector Network Analyzer

Measurements of the transmission coefficients of the samples was under taken at room temperature (25°C) using Agilent 8570B vector network analyser (VNA, Agilent Technologies, USA) at microwave frequency. For accuracy of measurement, the VNA was calibrated by using a two port calibration procedure at both ends of the coaxial cable. The OPEN, SHORT and LOAD calibration was carried out. After full calibration, standardize measurement of scattering parameter of air propagating through a rectangular wave guide was carried out. Good agreement of measurement value and that of manufacturers showed that calibration was accurate.

4. RESULTS AND DISCUSSION

4.1 Transmission Coefficient (S_{21})

Shown in Fig. 3 is are the measurement result for the transmission coefficients for the 15, 30 and 50 mm thick PTFE samples using VNA. Careful observation shows that more radiation is transmitted in the 15 mm thick sample at all frequency range.

Due to the amorphous nature of PTFE, less radiation were absorbed at frequency ranges for all samples. This amorphous nature makes it a poor transmitter of radiation when compared to compact materials. The behavior exhibited by PTFE is in agreement to the impedance mismatch theory for dense and less dense material [9]. It is noticed that the difference between the 15 and 30 mm thick PTFE is small compared to the 50 mm thick substrates. This disparity may be attributed to density and volume of thicker samples.

Further observation showed a sinusoidal wave like motion for the coefficients as the frequency increases which could also associated with the mismatch theory. The amorphous nature of PTFE may cause the inhomogeneity of the boundaries dislocation in its bulk which will tend to increase or decrease the transmission of the electromagnetic radiation depending on the thickness of the sample [10].

4.2 Comparison of Simulated and Measured Transmission Coefficients

Figs. 4-6, are the comparison for the measured and simulated transmission coefficients for the 15, 30 and 50 mm thick substrates. Observation shows that the measured and simulated quantities have the same qualitative behavior. Furthermore, the average value for the measured and simulated $|S_{21}|$ of 15 mm thick substrates are 0.46, and 0.50, respectively. For the 30 mm thick substrate, the values are 0.40 and 0.40, respectively and the 50 mm thick substrate had a value of are 0.19 and 0.16, respectively. The curve for measurement and simulation continued to decrease as frequency increases up to 12 GHz. At 10 GHz, the difference in the measured and simulated curve for $|S_{21}|$ is computed to be 0.05. Due to the agreement between the simulated and measured values of the transmission coefficient, it is believed that the data is suitable for visualizing the energy density of the materials hence the stopbands.

Based on the correlation of the measurement and simulation results, it is then concluded that the software "FEM" is suitable for electromagnetic characterization involving samples and line transmissions techniques. In addition, the correlation of the measured and simulated results confirms good measurement procedure which takes care of voids and gaps between the surface of samples and antenna surface.
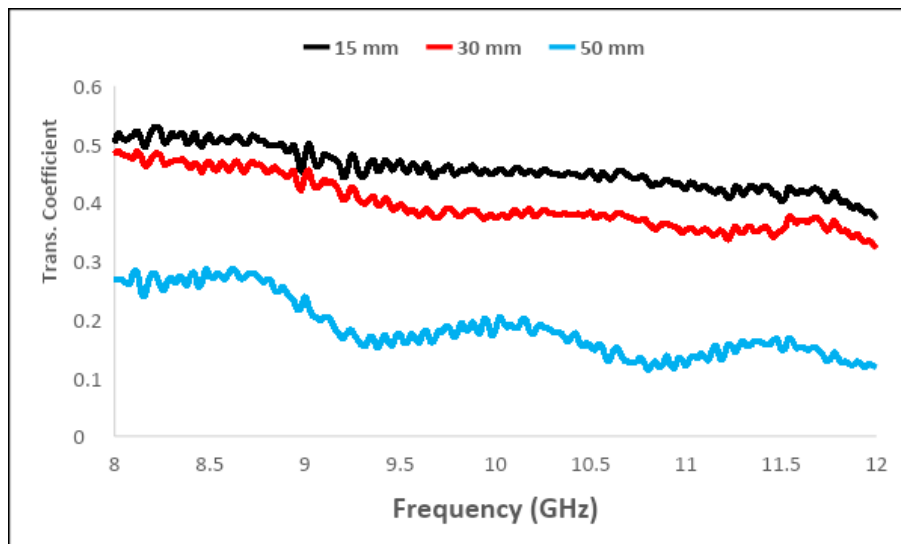

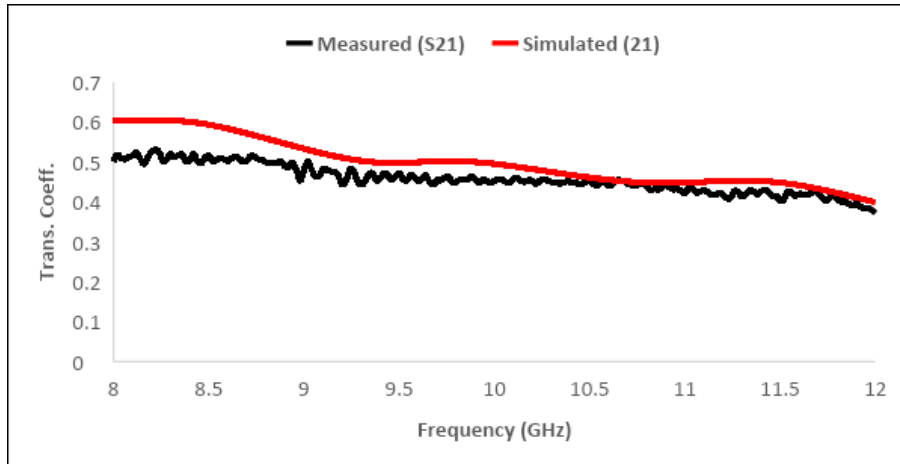**Fig. 3. Measured transmission coefficient for different substrates**

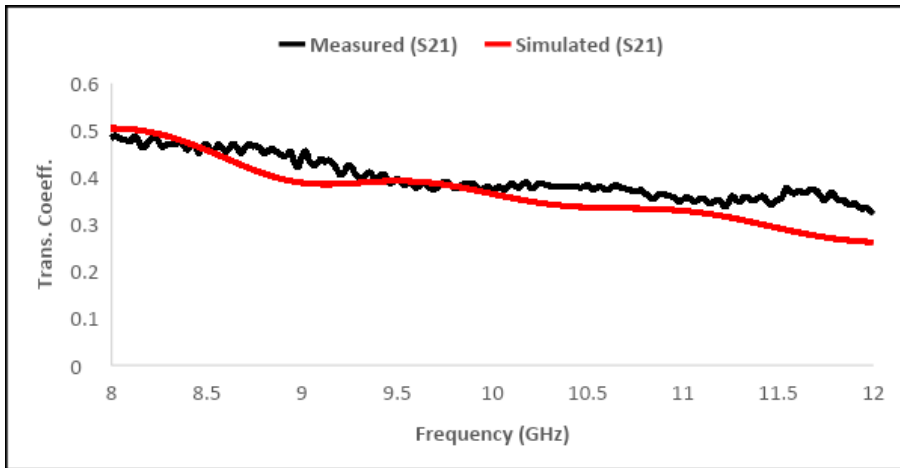**Fig. 4. Simulated and measured S_{21} for 15 mm thick PTFE**

Fig. 5. Simulated and measured S_{21} for 30mm thick PTFE
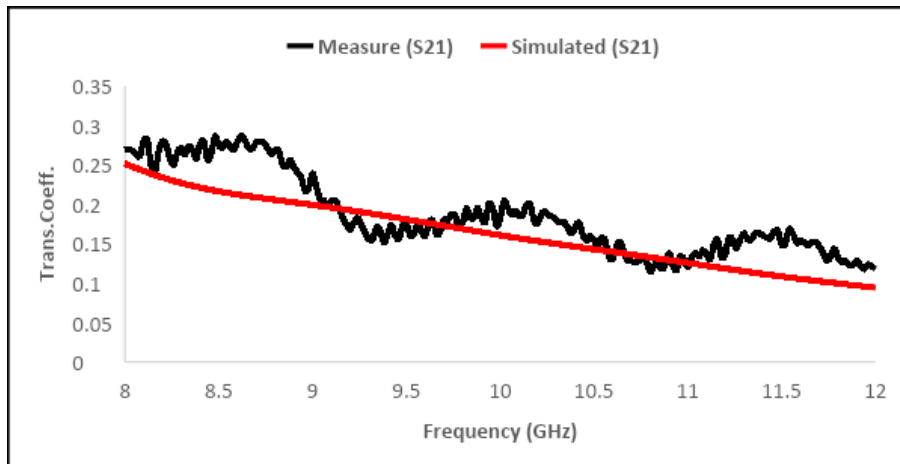

Fig. 6. Simulated and measured S_{21} for 50 mm thick PTFE

5

4.3 Energy Density Visualization Using Fem

Visualization of the total energy density was carried out using FEM from raw data of the transmission coefficients. Shown in Figs. 7 - 9 are the radiation flux of the energy density for the 15, 30 and 50 mm thick PTFE samples, respectively.

The energy density was determined to be 2.4 x 10^{-5} J/m^3 for the 15 mm thick substrate, 1.97 x 10^{-5} J/m^3 for the 30 mm thick PTFE and 1.67 x 10^{-5} J/m^3 for the 50 mm thick PTFE substrate. The close value between the energy density of the substrates were not surprising because energy density is the ratio of radiation intensity interacting with the substrate to its volume, which was computed by the software (FEM).

The attenuated power at 10 GHz for the 15 mm thick PTFE sample was calculated to be -6.8 dB while that of the 30 mm thick substrates was -8.0 dB and that of the 50 mm thick substrate was -14.6 dB. This result is also evident in the transmission coefficient value, where the 15 and 30 mm thick substrates difference was small compared to the 50 mm thick sample. This behavior as reported earlier is attributed to density and volume of the substrates.
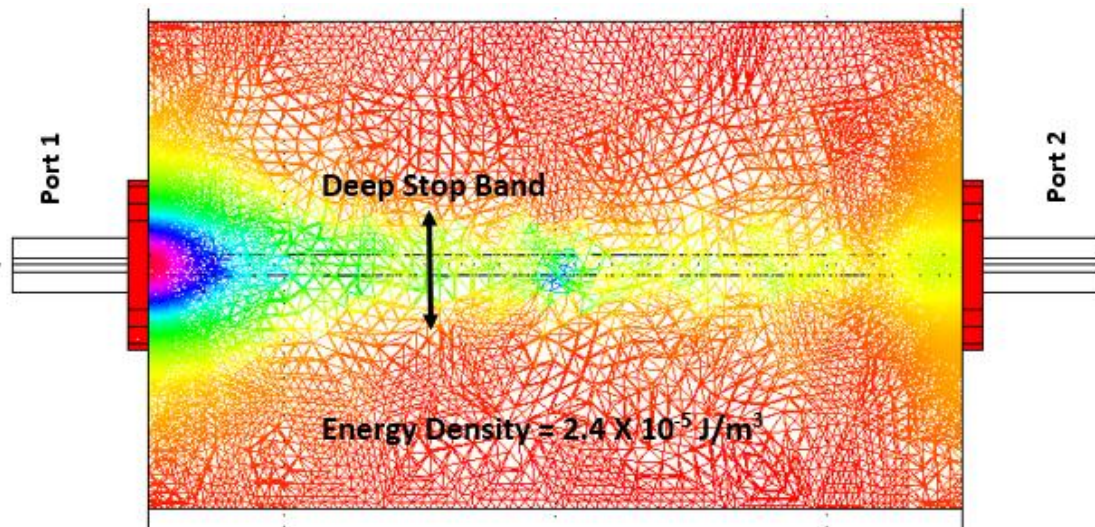

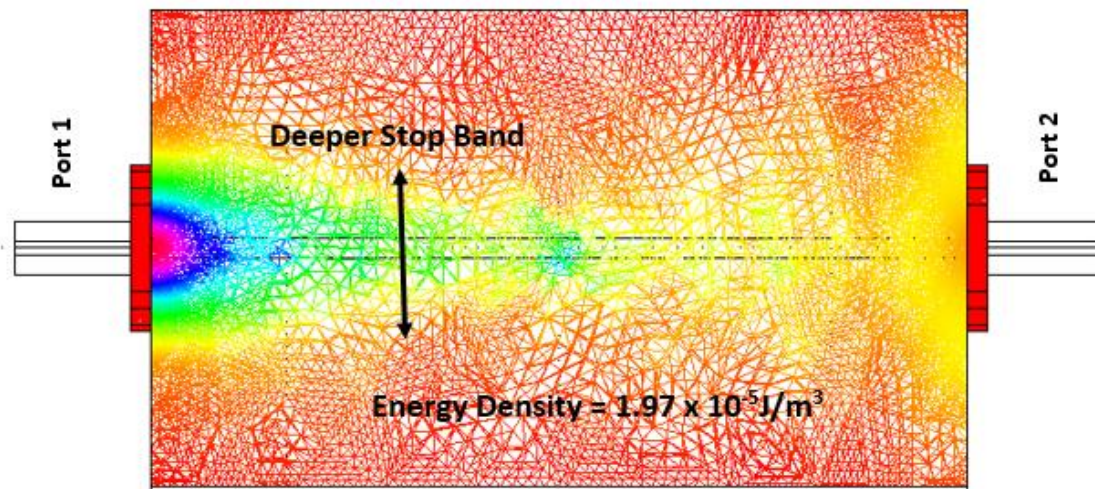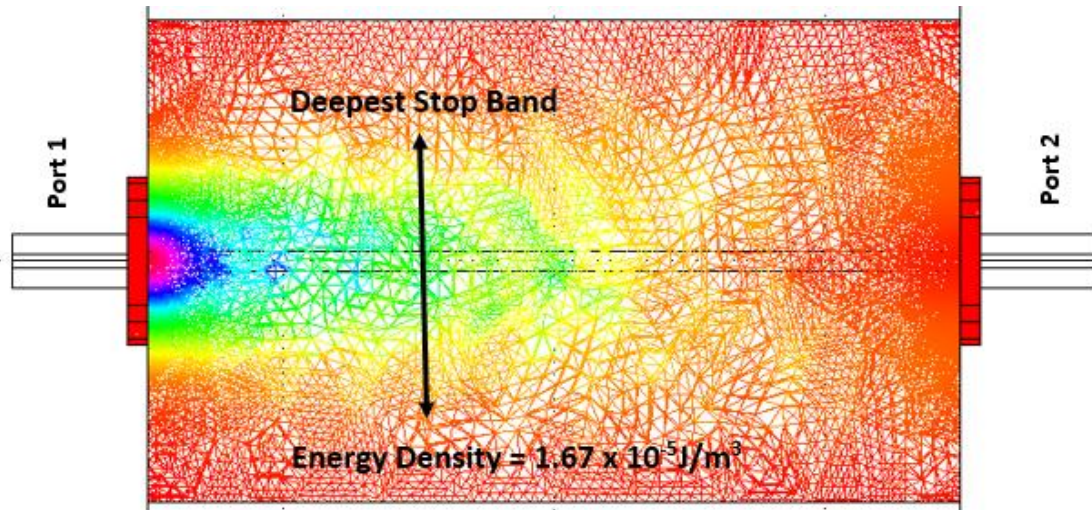**Fig. 7. Total energy density, time average for 15 mm thick PTFE**

**Fig. 8. Total energy density, time average for 30mm thick PTFE**

6

Fig. 9. Total energy density, time average for 50mm thick PTFE

The greenish, purple and pink colors in the plot represent the intensity of radiation calculated from simulated transmission coefficients, which has the same qualitative behavior as the radiation obtained from measurements. The width of radiation propagation around the strip-line from port 1 to 2 constitute the stopband. As expected, thicker samples gave rise to higher absorption of electromagnetic radiation, hence decrease in total energy density. The value of the stopband for the 50 mm thick substrate is in complete agreement with the result for the transmission coefficient and energy density for the same thickness. [11-12] reported stopband of -10.5 dB which is within the range of stopband visualize in this work.

Based on the visualize energy density, It is affirmed that the 50 mm thick PTFE substrates have the deepest stopband at 10 GHz and this result is in agreement with the visualized energy density with reference to radiation propagation from port 1 to port 2. This result is correlated to literature which reported that a 20 dB stop-band was obtained at a bandwidth of 13.2 GHz [13].
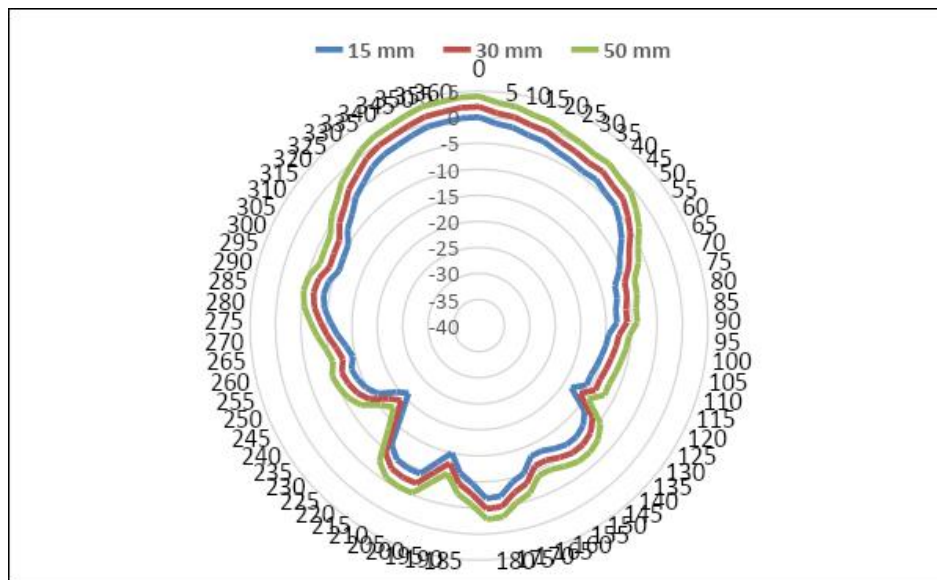
Fig. 10. Antenna gain pattern for substrates

Shown in Fig. 10 is the simulated radiation pattern of a microstrip antenna used in this work. The pattern is broad with low radiation power and broad frequency bandwidth. Results from the pattern suggests that an array of the antennas can be used to achieve greater directivity [14]. Careful observation shows that the antenna pattern has a back lobe which indicates low loss of energy during transmission. Based on findings, the radiation efficiency (gain) of antenna may be improved by larger substrates thicknesses.

5. CONCLUSION

In this work, simulation and measurement of transmission coefficient for the different thicknesses was done using FEM and VNA, respectively. Result obtained from both simulation and measurement were correlated and there was good amount of agreement between the methods. The energy density of the microstrip antenna were determined based on substrates used. From analysis, it is suggested that filters and antennas feeds could be designed using substrate thickness of material used in this work. This assertion is made based on the stopband of -6.8 to -14.6 dB attenuated power obtained. Further work can be carried out on the attenuation by representing it on a graph while the passband of feed designs can be visualize using FEM.

ACKNOWLEDGEMENT

COMPETING INTERESTS

Authors have declared that no competing interests exist.

REFERENCES

1. Yakubu A, Abbas Z, Abdullahi S. Mechanical, dielectric and shielding performance of rice husk/polycaprolactone composites enhanced via rice husk particles inclusion. Open Access Library Journal. 2020;7(e6514):1-12. Available:https://doi.org/10.4236/oalib.110 6514

2. Deyasi A, Debinath P, Bhattacharyya S. Applications of electromagnetic bandgap structure in microwave photonics. In Contemporary Developments in High-Frequency Photonic Devices. IGI Global. 2019;1-24.

3. Kumar A, Sharma S. Measurement of dielectric constant and loss factor of the dielectric material at microwave frequencies. Progress in Electromagnetics Research (PIER). 2007;69:47–54.

4. Hewlett Packard Company. HP 8719A, HP 8720B, Microwave Network Analyser Operating Manual; 1990.

5. Zulkifly A, Pollard RD, Kelsall RW. Complex permittivity measurements at ka-band using rectangular dielectric waveguide. IEEE Transactions on Instrumentation and Measurement. 2001; 50(5):1334-1342.

6. Belenguer A, Fernandez MD, Ballesteros JA, de Dios JJ, Esteban H, Boria VE. Compact multilayer filter in empty substrate integrated waveguide with transmission zeros. IEEE Transactions on Microwave Theory and Techniques. 2018; 66(6):2993-3000.

7. Kingsley S, Velan S, Kanagasabai M, Subbaraj S, Panneer Selvam Y, Balasubramaniyan B. Signal integrity analysis on a microstrip ultra-wideband coupled-line coupler. International Journal of Electronics. 2019;106(4):620-633.

8. Yakubu A, Zulkifli A, Mansor H. Effect of material thickness on attenuation (dB) of PTFE using finite element method at X-band frequency. Advances in Materials Science and Engineering. 2014;965912:5. Available:https://10.1155/2014/965912

9. Pozar DM. Microwave engineering, John Wiley & Sons, New-Jersey; 2012.

10. Sullivan AT. Layer thickness-dependent transition in the deformation mechanism of Ni-W amorphous-crystalline nano-laminates (Doctoral Dissertation, State University of New York at Stony Brook); 2018.

11. Roshani S, Roshani S, Zarinitabar A. A modified Wilkinson power divider with ultra-harmonic suppression using open stubs and lowpass filters. Analog Integrated Circuits and Signal Processing. 2019;98(2):395-399.

12. Golestanifar A, Roshani S. Design of an ultra-sharp composite low-pass filter using analytical method. Analog Integrated

Circuits and Signal Processing. 2019; 100(2):249-255.

13. Zhang X, Liu AQ, Karim MF, Yu AB, Shen ZX. Mems-based photonic bandgap (pbg) band-stop filter. 2004 IEEE MIT-s International Microwave Symposium Digest (IEEE cat. no.04ch37535), Fort Worth, TX, USA. 2004; 3:1463-1466.
DOI: 10.1109/mwsym.2004.1338849

14. Farahani S. RF propagation, antennas, and regulatory requirements. Zigbee Wireless Networks and Transceivers. 2008;1:171-206.